Fast and Wide-Range Wavelength Locking Based on a Two-Layer Neural Network in a Silicon Microring Switch

Qingming Zhu, Shaohua An, Ruiyuan Cao, Yuye Ling, and Yikai Su
State Key Laboratory of Advanced Optical Communication Systems and Networks, Department of Electronic Engineering, Shanghai Jiao Tong University, Shanghai 200240, China
Author e-mail address: yikaisu@sjtu.edu.cn

Abstract: We propose and experimentally demonstrate a neural-network-based wavelength locking algorithm for a 1 × 2 silicon microring switch. The wavelength locking is performed at a 20-nm/ms locking speed over a full free spectral range.
OCIS codes: (130.3120) Integrated optics devices; (130.4815) Optical switching devices; (230.5750) Resonators.

1. Introduction

Taking the advantages of high throughput, low latency and low power consumption, optical switching has attracted great attention in large-scale switching applications [1]. In a typical wavelength division multiplexed (WDM) switching network, the switch fabric consists of multiple wavelength layers, and each layer operates on a single wavelength [2]. To date, many photonic switch structures have been presented [3]. Among them, resonator-based switches are favored due to the compact footprint, low power consumption and sharp spectral selectivity [3]. However, the fabrication errors and chip temperature variations result in misalignments between the resonance wavelengths of such devices and the signal wavelengths [3]. Thus automated wavelength locking is required. Among the previously reported locking schemes, digital signal processing and associated algorithms have been widely employed for various device structures, including maximum/minimum searching [4], saddle point searching [5], gradient method [6], and so forth. These locking algorithms, however, exhibit relatively low locking speeds (e.g. 1.2 nm/ms [4], and 1.5 nm/ms [5]) resulting from the closed-loop control methods. As an alternative, open-loop control methods can speed up the control process whereas the deviations of the controlled variables may be increased [7]. To the best of our knowledge, open-loop wavelength locking algorithm for resonator-based switches has not been demonstrated.

In this paper, we experimentally demonstrate the automated wavelength locking of an O-band 1 × 2 silicon microring switch, with a high locking speed of 20 nm/ms over a full free spectral range (FSR) of 5.8 nm. To simultaneously achieve the high locking speed and wide locking range, an open-loop algorithm based on a two-layer neural network is proposed and implemented in an off-chip control sub-system. Compared to look-up tables, neural networks can significantly reduce the memory size and therefore solve high-dimensional problems [8]. The proposed algorithm is demonstrated at four different signal wavelengths over 6 nm. For all the signal wavelengths, wavelength locking is realized with a constant duration of 290 μs, and the locking errors are less than 0.05 nm.

2. Device structure and sub-system configuration

Fig. 1 presents the schematic configurations of the 1 × 2 switch and the control sub-system. The basic structure of the switch is an add-drop ring resonator, which can be tuned and locked to the input signal wavelength. A microheater, a p-i-n diode and a photodiode are integrated for thermo-optic (TO) tuning, electro-optic (EO) tuning and optical-to-electrical conversion, respectively. In the control sub-system, the converted photocurrent signal is amplified by a trans-impedance amplifier (TIA) and sampled by an analog-to-digital converter (ADC). The sampled signal is processed by the proposed algorithm to obtain the desired TO tuning power. A digital-to-analog converter (DAC) and a driver are then used to perform the TO tuning. Afterwards, fast switching is realized by the EO tuning.

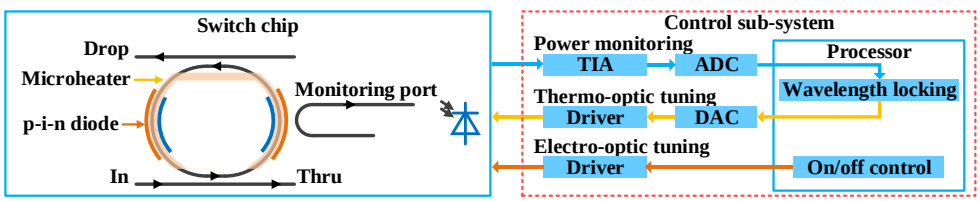

Fig. 1. Schematic configurations of the 1 × 2 switch and the control sub-system. TIA: trans-impedance amplifier.

3. Operation principle and algorithm design

The locking algorithm contains two stages, i.e., a training stage and a locking stage. In the training stage shown in Fig. 2(a), a two-layer neural network is used to learn the relation between the monitored optical powers and the

required TO tuning power. In detail, we first apply a set of TO tuning powers to the switch at a step denoted by $step_a$, and measure the corresponding monitored powers. The data set is then divided into M groups, where each group consists of three monitored powers and the spacing between the average TO tuning power of this group and the target TO tuning power. The three TO tuning powers in each group are spaced by $step_b$. The M groups are used to train the neural network. To achieve sufficient training, the M groups are sorted in a random order, and the training process is repeated by N epochs. After the training stage, the neural network can quickly predict the required TO tuning power for any wavelength shift within the FSR. As shown in Fig. 2(b), three TO tuning powers spaced by $step_b$ are applied to the switch, and the monitored optical powers are denoted by p_1, p_2, p_3, respectively. The three monitored powers are then sent to the neural network to obtain the required TO tuning power. Finally, the fourth TO tuning is performed to lock the ring resonator to the signal wavelength. The model of the neural network is depicted in Fig. 2(c). It is a fully connected neural network and contains a single hidden layer and an output layer. In the hidden layer, we use three functional neurons, which show a good trade-off between the predicted error and computational complexity. The training method is the standard error backpropagation (BP) algorithm [9], and the activation function of the neurons is the sigmoid function shown in Fig. 2(d). Note that although in principle a three-dimensional look-up table can provide the same function, $step_a$ should be much smaller to achieve the same locking accuracy, and the memory size increases exponentially.

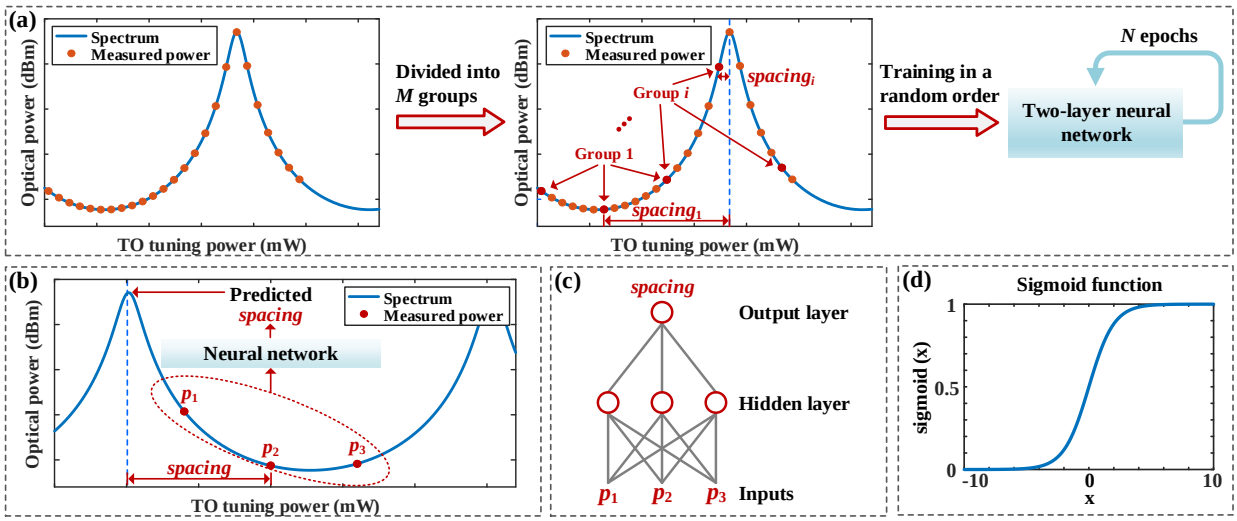

Fig. 2. (a) Illustration of the training stage. (b) Illustration of the locking stage. (c) Two-layer neural network model. (d) Activation function.

4. Experimental verifications

The schematic of the O-band 1 × 2 switch is depicted in Fig. 3(a). The ring resonator has a radius of 10 μm and an FSR of 5.8 nm, and the coupling gaps between the ring resonator and the straight waveguides are 200 nm. In the ring resonator, a ~98:2 directional coupler is used as a power monitoring port. The footprint of the switch is 674 μm × 604 μm. Fig. 3(b) shows the photograph of the experimental setup. The fabricated device is connected to the control circuits by wire bonding. Then a vertical coupling system is used to couple the lights into and out of the device, with a coupling loss of ~7 dB/facet. In the control circuits, the TIA has a gain of 2.5 × 10^5 V/A and a bandwidth of ~20 KHz. The ADC and DAC are integrated in a commercial processor (STM32F407), with a same quantization resolution of 12 bits and <5-μs conversion time. The locking algorithm and on-off control are implemented via C code. The maximal TO tuning power is set to 127 mW to achieve a 1.5-FSR tuning range. The thermal control period of the sub-system is set to 50 μs, mainly determined by the TO response time of the device.

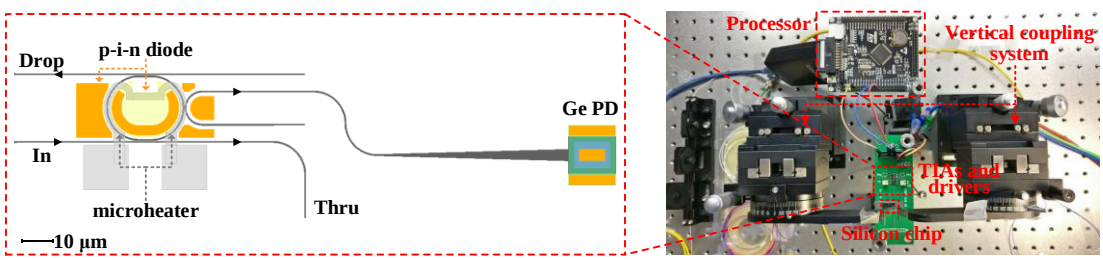

Fig. 3. (a) Schematic of the 1 × 2 silicon photonic switch. (b) Photograph of the experimental setup.

In the experiment, the training of the neural network is firstly performed at the signal wavelength of 1288 nm. The duration is 240 ms for 100 epochs. $step_a$ and $step_b$ are set to 2 mW and 24 mW, respectively. Hence, ~20 data groups can be obtained for the training. All the weights and thresholds of the neurons are initialized with random numbers from 0 to 1. Also, the learning rate in our neural network model is given by 20/sqrt(n_{epoch}), where n_{epoch} is the number of the current epoch. The predicted error of the required TO tuning power after each epoch is plotted in Fig. 4(a). After 100 epochs, the average predicted error can be reduced to <1 mW. Then we set four different signal wavelengths from 1288 nm to 1282 nm with a 2-nm step of the laser source. For each signal wavelength, a single locking process is carried out. Fig. 4(b) shows the monitored signal waveform during the locking process at 1288 nm as an example. The locking process contains four TO tuning operations and lasts for a constant time of 290 μs, thus achieving an average locking speed of 20 nm/ms. Fig. 4(c) shows the monitored photocurrents when the locking processes finished. The photocurrents are slightly lower than the recorded maxima, and the corresponding wavelength deviations are less than 0.05 nm. The above results are measured in short term, i.e., <1 ms, to avoid significant chip temperature drifts induced by large TO tuning powers. The normalized transmission spectra with and without the locking processes are also measured and plotted in Fig. 4(d). Without long-term stabilization, the maximal wavelength drift in the worst case is 0.25 nm. To achieve the long-term stabilization, a thermoelectric cooler (TEC) or a local maximum tracking algorithm [4] is required. Finally, fast switching is demonstrated by the EO tuning. As shown in Fig. 4(e), a 14.3-dB extinction ratio at the through port is achieved by applying an EO tuning power of 4.7 mW. The switching times for the rise edge and the fall edge are 4.5 ns and 4.0 ns, respectively.

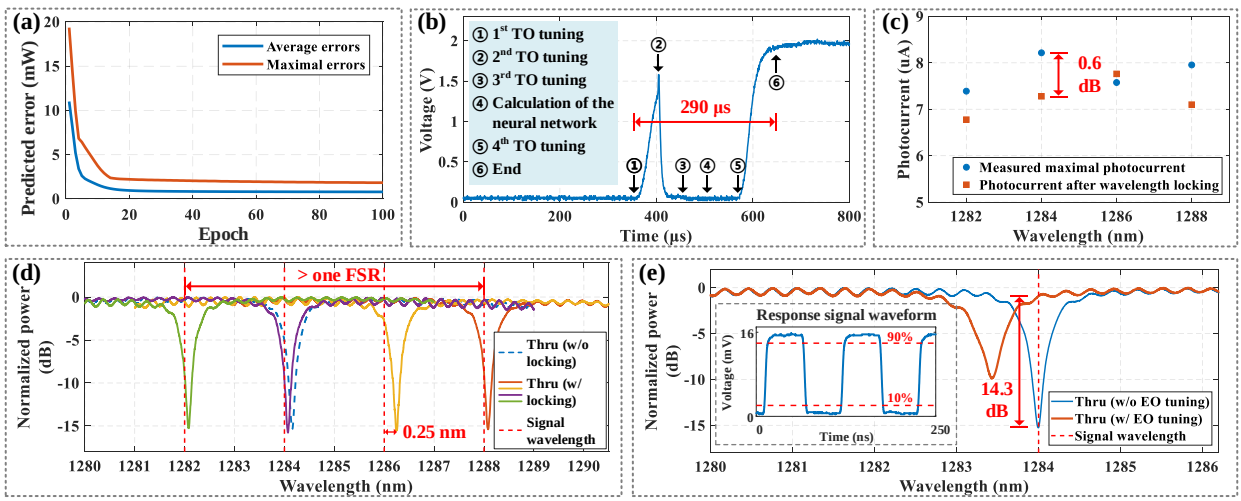

Fig. 4. (a) Predicted errors in the training process. (b) Monitored signal waveform. (c) Monitored photocurrents after locking. (d) Normalized transmission spectra with and without the locking processes. (e) Normalized transmission spectra with and without the EO tuning.

5. Conclusion

An automated wavelength locking algorithm based on a two-layer neural network is proposed and experimentally demonstrated for a 1 × 2 silicon microring switch. The algorithm can tune the resonance wavelength and lock the device to the signal wavelength over a full FSR of 5.8 nm with a constant duration of 290 μs, hence achieving a high locking speed of 20 nm/ms.

6. Reference

[1] G. I. Papadimitriou, C. Papazoglou, and A. S. Pomportsis, "Optical switching: Switch fabrics, techniques, and architectures," J. Lightw. Technol. **21**, 384-405 (2003).

[2] Q. Zhu, X. Jiang, Y. Yu, R. Cao, H. Zhang, D. Li, Y. Li, L. Zeng, X. Guo, Y. Zhang, and C. Qiu, "Automated wavelength alignment in a 4 x 4 silicon thermo-optic switch based on dual-ring resonators," IEEE Photon. J. **10**, 1-11 (2018).

[3] Y. Li, Y. Zhang, L. Zhang, and A. W. Poon, "Silicon and hybrid silicon photonic devices for intra-datacenter applications: state of the art and perspectives," Photon. Res. **3**, B10-B27 (2015).

[4] H. Jayatilleka, K. Murray, M. A. Guillen-Torres, M. Caverley, R. Hu, N. A. F. Jaeger, L. Chrostowski, and S. Shekhar, "Wavelength tuning and stabilization of microring-based filters using silicon in-resonator photoconductive heaters," Opt. Express **23**, 25084-25097 (2015).

[5] Q. Zhu, H. Zhang, R. Cao, N. Zhao, X. Jiang, D. Li, Y. Li, X. Song, X. Guo, Y. Zhang, and C. Qiu, "Wide-Range Automated Wavelength Calibration Over a Full FSR in a Dual-Ring based Silicon Photonic Switch," in Opt. Fiber Commun. Conf., 2018, Paper Th3C.1.

[6] R. Gatdula, K. Kim, A. Melikyan, Y. K. Chen, and P. Dong, "Simultaneous four-channel thermal adaptation of polarization insensitive silicon photonics WDM receiver," Opt. Express **25**, 27119-27126 (2017).

[7] B. C. Kuo, *Automatic Control Systems* (New Jersey: Prentice Hall, 1991), Chap. 6.

[8] A. H. Zaabab, "A neural network modeling approach to circuit optimization and statistical design," IEEE Trans. Microwave Theory Tech. **43**, 1349-1358 (1995).

[9] D. E. Rumelhart, G. E. Hinton, and R. J. Williams, "Learning representations by back-propagating errors," Nature **323**, 533–536 (1986).